Hidden order in URu_2Si_2: Symmetry-induced antitoroidal vortices

Vladimir E. Dmitrienko* and Viacheslav A. Chizhikov†

A.V. Shubnikov Institute of Crystallography, FSRC "Crystallography and Photonics" RAS, Leninskiy Prospekt 59, 119333, Moscow, Russia

(Received 8 September 2017; revised manuscript received 24 September 2018; published 11 October 2018)

We discuss possible approaches to the problem of the URu_2Si_2 "hidden order" (HO) which remains unsolved after tremendous research efforts. Suppose there is no spatial symmetry breaking at the HO transition temperature and solely the time-reversal symmetry breaking emerges owing to some sort of magnetic order. As a result of its $4/mmm$ symmetry, each uranium atom is a *three-dimensional* magnetic vortex; its intra-atomic magnetization $\mathbf{M}(\mathbf{r})$ is intrinsically noncollinear, so that its dipole, quadrupole, and toroidal moments vanish, thus making the vortex "hidden." The first nonzero magnetic multipole of the uranium vortex is the toroidal quadrupole. In the unit cell, two uranium vortices can have either the same or opposite signs of $\mathbf{M}(\mathbf{r})$; this corresponds to either *ferrovortex* or *antiferrovortex* structures with $I4/mmm$ or P_I4/mmm magnetic space groups, respectively. Our first-principles calculations suggest that the vortex magnetic order of URu_2Si_2 is rather strong: the total absolute magnetization $|\mathbf{M}(\mathbf{r})|$ is about $0.9\mu_B$ per U atom, detectable by neutron scattering in spite of the unusual form factor. The ferrovortex and antiferrovortex phases have almost the same energy and they are energetically favorable compared to the nonmagnetic phase.

DOI: 10.1103/PhysRevB.98.165118

I. INTRODUCTION

For more than 30 years, since the first papers appeared in 1985 [1–3], there were many attempts to understand the mysterious hidden order (HO) in the heavy-fermion compound URu_2Si_2 (they are surveyed in two detailed reviews [4,5]). The main problem is that below the HO transition temperature, $T_{HO} = 17.5$ K, there are practically no obvious physical phenomena associated with the order parameter; the only unequivocal evidence for the order is a rather strong specific heat jump [1–3] at T_{HO}. For instance, the accompanying antiferromagnetic order violating the body-centered symmetry [6–9] is so weak that it cannot explain the behavior of the specific heat. The observed lattice symmetry breaking [10] and in-plane anisotropy of the magnetic susceptibility [11] are also extremely weak and their relation to HO is not clear [12]. The symmetry breaking from body-centered tetragonal to simple tetragonal was carefully examined [13] via inelastic neutron and x-ray scattering measurements, and no signs of reduced spatial symmetry, even in the HO phase, had been found. The fourfold local symmetry of the HO state of URu_2Si_2 has recently been confirmed by means of single-crystal NMR measurements [14].

There have been several interesting attempts to understand the HO transition within the phenomenological Landau-Ginzburg theory (see, for instance, [15–18], and references therein). The phenomenological approaches include naturally both the hidden order and the pressure-dependent antiferromagnetic order. They also take into account the results of *ab initio* studies. However, for the time being, the problem is still very open, and we also discuss other possible forms of the order parameter in this paper.

A popular idea is that there is time-reversal symmetry breaking (TRSB) related probably with an exotic type of multipole magnetic order emerging at T_{HO} [5,19,20]. Many efforts, theoretical and experimental, were concentrated on searching for possible multipole orders [5,21–26]. However, the conventional methods such as magnetic neutron and resonant x-ray scattering seem unable to detect those multipoles.

In this paper, we suggest a simple HO model based mainly on the symmetry consideration. Indeed, if we cannot detect any pronounced violation of the *spatial* symmetry below T_{HO}, let us assume that the HO has exactly the same symmetry, namely, $4/mmm$, as the high-temperature paramagnetic phase of URu_2Si_2. More precisely, we suppose that HO is a noncollinear intra-atomic magnetization of uranium atoms with $4/mmm$ symmetry so that the only symmetry violation at the transition point is TRSB. Surprisingly, such a simple assumption leads to a nontrivial vortex HO described by the toroidal quadrupole order parameter which is difficult to detect with conventional methods. First-principles calculations show that the vortex HO is perhaps strong enough to be detected by careful monitoring of neutron reflections across the phase transition.

II. MAGNETIC SYMMETRY OF THE HIDDEN ORDER

We first remind one that the magnetic moment $\mathbf{M}(\mathbf{r})$ is a pseudovector and transformations of its components under mirror reflections are just opposite to a usual vector: the component normal to the mirror plane keeps its direction, whereas the parallel components invert their directions. For instance, for the m_z mirror plane, $M_z(x, y, -z) = M_z(x, y, z)$, $M_x(x, y, -z) = -M_x(x, y, z)$, and $M_y(x, y, -z) = -M_y(x, y, z)$. The space inversion

*dmitrien@crys.ras.ru
†chizhikov@crys.ras.ru

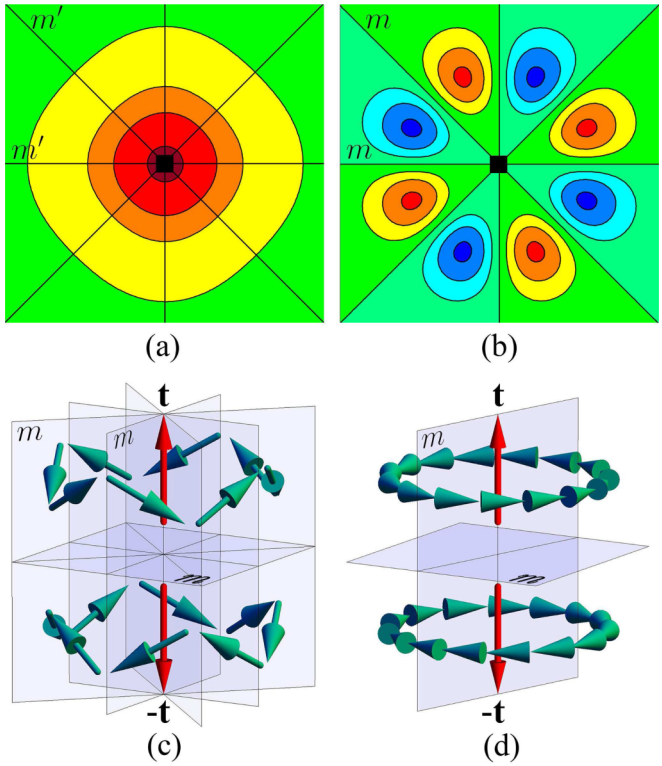

FIG. 1. Different symmetries of intra-atomic magnetization of uranium atoms in URu_2Si_2. (a) A conventional magnetic atom would have the point symmetry $4/mm'm'$ including the vertical fourfold axis (black square), the horizontal mirror plane m (the figure plane), and two types of vertical pseudomirror planes m' (perpendicular to the x or y axes and diagonal to them; black lines); m' means a combined operation of mirror reflection and time reversal. (b) In-plane uranium magnetization with the $4/mmm$ symmetry where red and blue colors correspond to positive and negative regions of $M_z(x, y, z = 0)$ divided by mirror planes m (black lines). (c) Three-dimensional ATV: sixteen $4/mmm$-equivalent magnetic vectors (green arrows) form two 8-vector vortices at $\pm z$ with opposite directions of toroidal moments (red arrows); see also a movie in Ref. [27]. It should be emphasized that the $4/mmm$ symmetry induces the ATV structure only for pseudovectors like $\mathbf{M}(\mathbf{r})$ and not for true vectors like electric dipole moments, etc. (d) In principle, higher symmetries are also possible, up to ∞/mm, which is the symmetry of the nematic order.

does not change $\mathbf{M}(\mathbf{r})$: $\mathbf{M}(-\mathbf{r}) = \mathbf{M}(\mathbf{r})$. The time-reversal symmetry operation, denoted by the prime sign, inverts the direction of the magnetization: $\mathbf{M}'(\mathbf{r}) = -\mathbf{M}(\mathbf{r})$.

The principal difference between conventional magnetic atoms and a magnetic atom with $4/mmm$ symmetry is obvious from Fig. 1. The magnetic point symmetry of conventional atoms would be $4/mm'm'$ and it includes one vertical fourfold axis, one horizontal mirror plane m, and two types of vertical mirror planes m' (normal and diagonal to the x, y axes). As a result of this symmetry, $M_x(x, y, 0) = 0$ and $M_y(x, y, 0) = 0$ in the $z = 0$ mirror plane and usually these components remain to be small above and below the mirror plane so that the main magnetization of the atom is M_z.

For the case of $4/mmm$ symmetry, M_x and M_y are also zero in the plane of the figure but M_z should be very inhomogeneous; it should change its sign at least eight times when we go around the atom [Fig. 1(b)]. In the horizontal mirror plane $z = 0$, we have eight similar sectors with alternating M_z component. Then, passing through all vertical mirror planes, shown in Fig. 1(b) by black lines, the parallel components of $\mathbf{M}(\mathbf{r})$ become zero and change their signs. In other words, for all $\mathbf{r}$ belonging to the mirror planes of $4/mmm$ symmetry, $\mathbf{M}(\mathbf{r})$ is normal to the corresponding plane.

For any general position x, y, z the $4/mmm$ symmetry operations create a pair of eight-vector vortices with head-to-tail arrangement of *equivalent* moments in the $\pm z$ planes [Fig. 1(c)]. The toroidal moments [28–30] of these two eight-vector vortices are antiparallel (along $\pm\mathbf{z}$). It is a general magnetic arrangement dictated by the $4/mmm$ symmetry and it makes the $\mathbf{M}(\mathbf{r})$ field significantly noncollinear and inhomogeneous simply as a result of the symmetry. Each uranium atom looks like an atomic-size magnetic skyrmion built from two equivalent halves at $z > 0$ and $z < 0$ with opposite toroidal moments. We could refer to this configuration as an antitoroidal vortex (ATV). It should be emphasized that the $4/mmm$ symmetry induces the ATV HO only for pseudovectors such as $\mathbf{M}$ and not for true vectors such as electric dipole moments, etc.

To characterize quantitatively the inhomogeneous atomic magnetization with $4/mmm$ point symmetry we can use the tensor moments of $\mathbf{M}(\mathbf{r})$ relative to the atomic center. The average dipole moment $\langle\mathbf{M}(\mathbf{r})\rangle$ is zero. Here and below $\langle\cdots\rangle$ means integration $V^{-1}\int\cdots d\mathbf{r}$ over a spherical atomic-size volume V around the atom. The magnetic quadrupole moment $\langle M_i(\mathbf{r})x_j\rangle = 0$ because of the inversion center $\mathbf{M}(-\mathbf{r}) = \mathbf{M}(\mathbf{r})$. In particular, the atomic toroidal (anapole) moment $\langle[\mathbf{r}\times\mathbf{M}(\mathbf{r})]\rangle$ [28–30], which is an antisymmetric part of this tensor, is zero as well as the monopole moment $\langle\mathbf{r}\cdot\mathbf{M}(\mathbf{r})\rangle$. For the same reason, all even-rank tensor moments of $\langle M_i(\mathbf{r})x_j\cdots x_n\rangle$ type are zero as well.

Thus the first nonzero tensor moment of the $4/mmm$ ATV structure is the third-rank tensor $M_{ijk} = \langle M_i(\mathbf{r})x_jx_k\rangle$; it is symmetric under permutation of the last two indices. It is easy to show (or to find in textbooks [31]) that for this symmetry the third-rank pseudotensor M_{ijk} has only four nonzero components and all of them are equal up to the sign $M_{123} = M_{132} = -M_{231} = -M_{213} = M_v$, where $M_v = \frac{1}{2}V^{-1}\int[\mathbf{M}(\mathbf{r})\times\mathbf{r}]\cdot\mathbf{z}\,d\mathbf{r}$. The time-odd parity-even moment M_v characterizes the strength and sign of the ATV HO (it is called either magnetic octopole or quadrupole toroidal moment).

The sign of M_v is a nontrivial attribute. Indeed, we can change the sign of M_v by reversing the magnetization direction in all points $\mathbf{M}(\mathbf{r}) \to -\mathbf{M}(\mathbf{r})$ (the time-reversal operation). However, this way we obtain a new object which cannot be superposed with the old one either by rotations or by mirror reflections. Since the only symmetry operation relating these two objects is the time inversion, their energies must be equal. Thus any magnetization arrangement with $4/mmm$ point symmetry can exist in two energetically equivalent variants with $\pm M_v$. It is natural to call them clockwise and anticlockwise vortices for $M_v > 0$ and $M_v < 0$, correspondingly. However, it should be emphasized that the sign of M_v is not

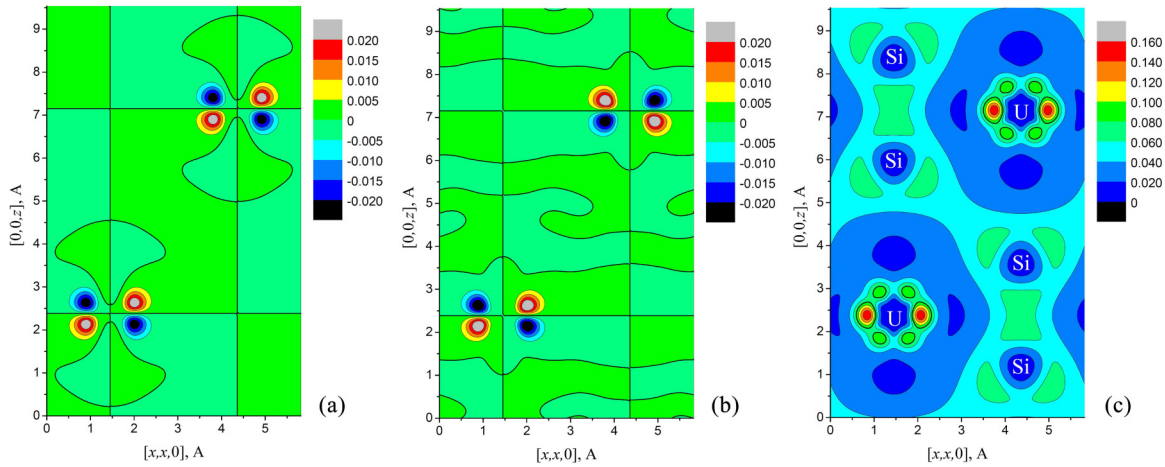

FIG. 2. The calculated magnetization distribution $M_x(\mathbf{r})$ within the diagonal mirror plane formed by vectors [1,1,0] and [0,0,1] in the unit cell of the ferrovortex (a) and antiferrovortex (b) phases; (c) the calculated valence electron density which is almost equal for both phases. In this plane, $M_y(\mathbf{r}) = -M_x(\mathbf{r})$ and $M_z(\mathbf{r}) = 0$. Two uranium atoms are at $(\frac{1}{4}, \frac{1}{4}, \frac{1}{4})$ and $(\frac{3}{4}, \frac{3}{4}, \frac{3}{4})$ positions with Si atoms surrounding them; Ru atoms are out of the plane. The straight lines are intersections with vertical and horizontal mirror planes where M_x and M_y change their signs.

topologically stable; it can be changed by deformation of the $\mathbf{M}(\mathbf{r})$ field. The magnetization arrangement with $M_v = 0$ can correspond to nonzero absolute magnetization $\langle|\mathbf{M}(\mathbf{r})|\rangle \neq 0$.

There are two uranium atoms in the body-centered-tetragonal unit cell of URu_2Si_2. In the simplest magnetic structure, both atoms have the vortices with the same M_v, either both clockwise or both anticlockwise. Such structure has the $I4/mmm$ magnetic space group [32,33] and can be called the ferrovortex phase. The clockwise and anticlockwise ferrovortex phases should have equal energies and can be mutually transformed by the time reversal. The clockwise and anticlockwise domains can coexist, being separated by domain walls, in real samples of the ferrovortex phase.

If those two atoms have opposite magnetization directions (one clockwise and another anticlockwise), then the lattice is primitive and the magnetic symmetry group is P_I4/mmm [32,33]. In this case, the lattice consists of clockwise and anticlockwise layers alternating along the z axis; it can be called the antiferrovortex phase. The time reversal is equivalent to the $(\frac{1}{2}, \frac{1}{2}, \frac{1}{2})$ shift of the lattice.

Besides ferrovortex and antiferrovortex phases, many (infinite) symmetrically different arrangements of the clockwise and anticlockwise vortices are possible but their consideration should be left for a future work. Then, in principle, ATV with higher symmetries are also possible, up to ∞/mm, which is the symmetry of the nematic order [see Fig. 1(d)]. An open question is whether the vortices with such a high symmetry can exist in free atoms, molecules, or nematiclike liquid crystals. Actually, the toroidal quadrupole moments are discussed for positronium atoms [34] and for deuterons [35] (a survey of related works is given in [36]).

The quantitative characterization of $4/mmm$ vortices by the third-rank tensor M_{ijk} has three important complications: (i) M_{ijk} does not depend on the azimuthal orientation of the vortex in the xy plane: (ii) it does not distinguish between $4/mmm$ and other uniaxial symmetries (422, $4mm$, $\bar{4}2m$, 622, $6mm$, $\bar{6}2m$, $6/mmm$, $\infty 2$, ∞m, ∞/mm); (iii) the M_z component gives no contribution to M_v. Some of these drawbacks disappear for the next nonzero tensor (fifth rank) and for the magnetoelectric tensor $\langle M_i(\mathbf{r})E_j(\mathbf{r})x_k\rangle$. All this means that pure symmetrical consideration leaves a lot of freedom for possible scenarios of the HO transition and more work is needed here.

III. FIRST-PRINCIPLES SIMULATIONS

The symmetry-based approach is of course reliable, but it cannot say whether and when those exotic antitoroidal vortices could be energetically stable, what are the values of $\mathbf{M}(\mathbf{r})$ in different points of the unit cell, etc. To find the magnetization $\mathbf{M}(\mathbf{r})$, the electronic densities $\rho(\mathbf{r})$, and the energies of possible URu_2Si_2 phases we have performed "illustrative" *ab initio* simulations using the QUANTUM ESPRESSO package [37,38] with appropriate pseudopotentials and techniques [39–47].

We do not fix the spatial and magnetic symmetries of URu_2Si_2 in the beginning and during the self-consistent minimization procedure. Instead, the procedure starts from crystal structures whose symmetries are subgroups of $I4/mmm$. Small initial magnetic moments are assigned to silicon and ruthenium atoms so that uranium magnetic moments are not predetermined. Then during the self-consistent iterations those conventional magnetic moments become smaller and smaller but at the same time a new magnetization field $\mathbf{M}(\mathbf{r})$ (with zero average magnetization) is growing mainly around uranium atoms, i.e., the absolute magnetization $\langle|\mathbf{M}(\mathbf{r})|\rangle$ is progressively growing until an equilibrium structure is reached. Symmetry analysis of the appearing magnetization shows that new symmetry elements initially look like some tendency and then become more and more exact if the iterative self-consistent procedure converges. See Ref. [48] for more details of the simulations.

Both the ferrovortex and antiferrovortex phases have been obtained in our simulations starting from different initial structures. Their energies are well below the energy of the nonmagnetic phase: per formula unit, $\Delta E_{fv} =$

-0.0318 eV/f.u. and $\Delta E_{av} = -0.0364$ eV/f.u. This energy gain seems to be too strong for the observed value [1–3] of the specific heat jump corresponding to the internal energy change induced by the hidden order of about 0.000 18 eV/f.u. In fact, the energy responsible for the HO phase transition is of about an *interaction energy* between magnetic atoms, which is "fighting" with entropy for the phase transition. The interaction energy is a very small part of the total magnetic energy and the former is impossible to extract from the latter within the conventional density-functional theory simulations. Quite probably, the antitoroidal vortices appear as fluctuations well above the HO transition temperature, and they are arranged into ferrovortex or antiferrovortex phase at the HO transition temperature owing to very subtle interactions between vortices.

The calculated magnetization and charge densities are shown in Fig. 2 for the diagonal mirror plane $x = y$ including two U atoms. The main magnetic and charge features obviously correspond to the $5f$ uranium orbitals [49] (mean radius 0.76 Å). The uranium vortices are almost the same for both phases, except that in the antiferrovortex phase they have opposite signs. And the total absolute magnetization is almost the same for both phases: $|\mathbf{M}(\mathbf{r})_{fv}| = 0.93\mu_B$/f.u. and $|\mathbf{M}(\mathbf{r})_{av}| = 0.96\mu_B$/f.u. According to Ref. [50], the value of about $1\mu_B$/f.u. is needed to explain the observed specific heat jump. The magnetization is concentrated around uranium atoms [Figs. 2(a) and 2(b)]: in the ferrovortex (antiferrovortex) phase, there is about 0.936 (0.93) of the total $|\mathbf{M}(\mathbf{r})|$ inside the Slater uranium radii ($R_S = 1.75$ Å) and remaining itinerant magnetization is distributed in the unit cells according to their space symmetries. The very strong anisotropy of ATVs could naturally explain the Ising-like behavior of HO [5,12]. The calculated M_z for one atom is shown in Fig. 1(b) which is a 0.5×0.5 part of the unit cell xy plane (i.e., about 2×2 Å^2); see also movies in Ref. [51].

In fact, it is well known that magnetic intra-atomic noncollinearity is a general effect, arising because of the relativistic spin-orbit coupling not only in actinides [52] but also in other materials [53–55]. The noncollinear magnetism is very sensitive to the space group symmetry and we have predicted recently [56] the toroidal intra-atomic moments for RhGe crystal with the $P2_13$ space group. The case of URu_2Si_2 is especially interesting because its symmetry is so high that observation of its intra-atomic vortices is really a nontrivial problem.

IV. DISCUSSION

The logic of our approach is straightforward:

(i) To explain the observed large anomaly in the specific heat of URu_2Si_2, we need a rather strong order.

(ii) To be hidden, the strong order should have the symmetry of the high-temperature phase, because otherwise it would be easily detectable by x-ray and/or neutron diffraction.

(iii) If the order parameter has the symmetry of the high-temperature phase, the phase transition should be (contrary to experiments) of the first order except for the case of the time-reversal-symmetry breaking. Therefore the most plausible candidate for the "hidden order" in URu_2Si_2 is a time-reversal-symmetry breaking system of magnetic moments with the symmetry of the crystal lattice. In our version, this is the tetragonal lattice of antitoroidal vortices.

(iv) This conjecture has been fully confirmed in our *ab initio* calculations.

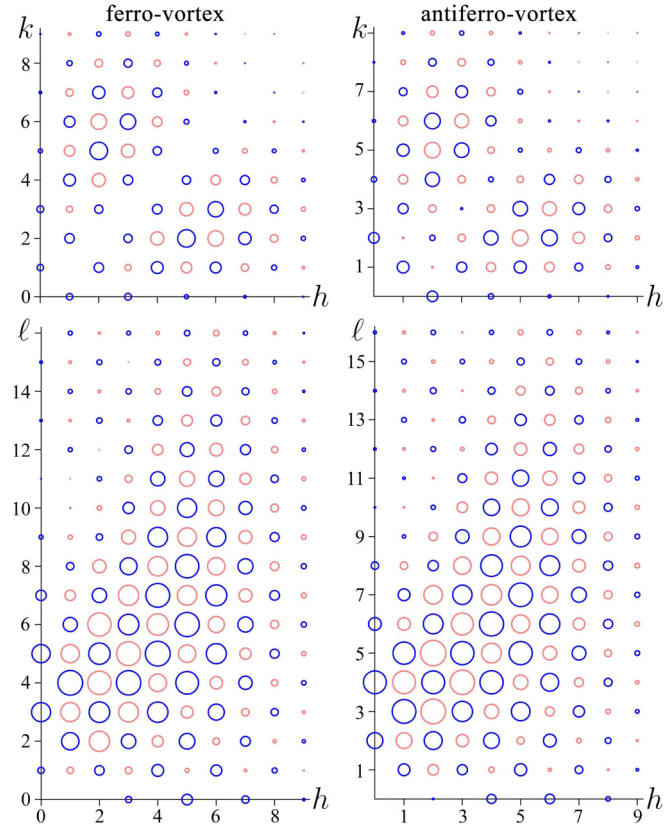

FIG. 3. Relative intensities of magnetic contributions to neutron reflections for the ferrovortex ($h + k + \ell = 2n$, left) and antiferrovortex ($h + k + \ell = 2n + 1$, right) phases; the circle areas are proportional to $|\mathbf{M}(hk\ell)|^2$ and normalized on the most intense magnetic reflections, 255 and 256 for the ferrovortex and antiferrovortex phases, respectively. Top: for $hk0$ (red) and $hk1$ (blue). Bottom: for $h0\ell$ (red) and $h1\ell$ (blue). The antitoroidal magnetization of uranium atoms [Figs. 2(a) and 2(b)] results in a rather unusual reciprocal-space distribution of strong reflections: magnetic contributions are zero for $h00$, $0k0$, 00ℓ, and $hh0$ reflections.

Now we want to show that the hidden order of this type can be detected means of careful monitoring of neutron reflections across the HO phase transition. It is helpful that the lattice symmetry favors the ATV HO with very unusual distributions of the intra-atomic magnetization resulting in unusual form factors for magnetic neutron scattering [see Fig. 3 for the reflection intensities obtained from *ab initio* calculated $\mathbf{M}(\mathbf{r})$]. An obvious unusual feature is that high-symmetry reflections $h00$, $0k0$, 00ℓ, and $hh0$ are zero for both the ferrovortex and antiferrovortex phases. The main difference between the two phases is that there are pure magnetic reflections $h + k + \ell = 2n + 1$ in the antiferrovortex phase, whereas for the ferrovortex phase all the magnetic reflections coincide with nuclear reflections $h + k + \ell = 2n$. A comparison of Fig. 3 with the observed intensities of pure magnetic reflections [8] (100, 102, 201, 203, 106, and 300) allows us to exclude

the antiferrovortex phase from the list of possible candidates for HO.

The situation with the ferrovortex phase is much more intriguing: the magnetic reflections only slightly change the nuclear reflection intensities; the latter have never been measured carefully for URu_2Si_2 across the HO temperature. Moreover, the interference between magnetic and nuclear contributions should vanish in the case of equal fractions of clockwise and anticlockwise domains. According to our calculations, the magnetic structure factor can reach its maximum $\approx 0.25\mu_B$ for reflection 525 at $T = 0$. However, this reflection has a large nuclear structure factor. Fortunately, there are many weak nuclear reflections with comparable magnetic factors from 0.15 to $0.2\mu_B$; for instance, 307 and 417; they are more sensitive to magnetic scattering. It seems that accurate measurements of neutron reflections as a function of temperature provide the only way to study ATV HO quantitatively. Similar neutron experiments have revealed an unusual magnetic order preserving translational symmetry of the lattice in the enigmatic pseudogap phase of high-temperature superconductors [57–61]. We have found recently a striking similarity between hidden orders in URu_2Si_2 and in the pseudogap phase that will be discussed elsewhere. Quite probably, the URu_2Si_2 HO phase is generic and similar phases where the order remains undetected because of its high symmetry can exist in other materials.

In conclusion, it is shown that high magnetic symmetry of URu_2Si_2 crystal can explain why its hidden order remains hidden for many years. There is no spatial symmetry breaking in the HO phase transition and solely the time-reversal symmetry is violated. Owing to their $4/mmm$ symmetry, uranium atoms have zero dipole and quadrupole moments, and the first nonzero magnetic moment of the uranium vortex is the quadrupole toroidal moment which can be used as an order parameter in the Landau theory of the HO phase. The simulations suggest that the vortex magnetic order of URu_2Si_2 is indeed energetically favorable and strong enough to be detected by neutron diffraction.

ACKNOWLEDGMENTS

We are grateful to S. A. Pikin, M. V. Gorkunov, F. de Bergevin, G. Beutier, R. Caciuffo, S. P. Collins, M. Kléman, Y. O. Kvashnin, N. V. Ter-Oganesyan, and I. V. Tokatly for useful discussions and communications. This work was supported by the Ministry of Science and Higher Education of the Russian Federation within the State assignment FSRC "Crystallography and Photonics" RAS in part for symmetry analysis, and by the Grant of Prezidium RAS No. I.П.08 "Condensed matter physics and materials of new generation" in part for *ab initio* calculations.

[1] T. T. M. Palstra, A. A. Menovsky, J. van den Berg, A. J. Dirkmaat, P. H. Kes, G. J. Nieuwenhuys, and J. A. Mydosh, Superconducting and Magnetic Transitions in the Heavy-Fermion System URu_2Si_2, Phys. Rev. Lett. **55**, 2727 (1985).

[2] M. B. Maple, J. W. Chen, Y. Dalichaouch, T. Kohara, C. Rossel, M. S. Torikachvili, M. W. McElfresh, and J. D. Thompson, Partially Gapped Fermi Surface in the Heavy-Electron Superconductor URu_2Si_2, Phys. Rev. Lett. **56**, 185 (1986).

[3] W. Schlabitz, J. Baumann, B. Pollit, U. Rauchschwalbe, H. M. Mayer, U. Ahlheim, and C. D. Bredl, Superconductivity and magnetic order in a strongly interacting fermi-system: URu_2Si_2, Z. Phys. B **62**, 171 (1986).

[4] J. A. Mydosh and P. M. Oppeneer, *"Colloquium*: Hidden order, superconductivity, and magnetism: The unsolved case of URu_2Si_2," Rev. Mod. Phys. **83**, 1301 (2011).

[5] J. A. Mydosh and P. M. Oppeneer, Hidden order behaviour in URu_2Si_2 (A critical review of the status of hidden order in 2014), Philos. Mag. **94**, 3642 (2014).

[6] C. Broholm, J. K. Kjems, W. J. L. Buyers, P. Matthews, T. T. M. Palstra, A. A. Menovsky, and J. A. Mydosh, Magnetic Excitations and Ordering in the Heavy-Electron Superconductor URu_2Si_2, Phys. Rev. Lett. **58**, 1467 (1987).

[7] E. D. Isaacs, D. B. McWhan, R. N. Kleiman, D. J. Bishop, G. E. Ice, P. Zschack, B. D. Gaulin, T. E. Mason, J. D. Garrett, and W. J. L. Buyers, Buyers, X-ray Magnetic Scattering in Antiferromagnetic URu_2Si_2, Phys. Rev. Lett. **65**, 3185 (1990).

[8] C. Broholm, H. Lin, P. T. Matthews, T. E. Mason, W. J. L. Buyers, M. F. Collins, A. A. Menovsky, J. A. Mydosh, and J. K. Kjems, Magnetic excitations in the heavy-fermion superconductor URu_2Si_2, Phys. Rev. B **43**, 12809 (1991).

[9] H. C. Walker, R. Caciuffo, D. Aoki, F. Bourdarot, G. H. Lander, and J. Flouquet, Resonant X-ray scattering study of the URu_2Si_2 hidden-order phase, Phys. Rev. B **83**, 193102 (2011).

[10] S. Tonegawa, S. Kasahara, T. Fukuda, K. Sugimoto, N. Yasuda, Y. Tsuruhara, D. Watanabe, Y. Mizukami, Y. Haga, T. D. Matsuda, E. Yamamoto, Y. Onuki, H. Ikeda, Y. Matsuda, and T. Shibauchi, Direct observation of lattice symmetry breaking at the hidden-order transition in URu_2Si_2, Nat. Commun. **5**, 4188 (2014).

[11] R. Okazaki, T. Shibauchi, H. J. Shi, Y. Haga, T. D. Matsuda, E. Yamamoto, Y. Onuki, H. Ikeda, and Y. Matsuda, Rotational symmetry breaking in the hidden-order phase of URu_2Si_2, Science **331**, 439 (2011).

[12] J. Trinh, E. Brück, T. Siegrist, R. Flint, P. Chandra, P. Coleman, and A. P. Ramirez, Thermodynamic Measurement of Angular Anisotropy at the Hidden Order Transition of URu_2Si_2, Phys. Rev. Lett. **117**, 157201 (2016).

[13] N. P. Butch, M. E. Manley, J. R. Jeffries, M. Janoschek, K. Huang, M. B. Maple, A. H. Said, B. M. Leu, and J. W. Lynn, Symmetry and correlations underlying hidden order in URu_2Si_2, Phys. Rev. B **91**, 035128 (2015).

[14] S. Kambe, Y. Tokunaga, H. Sakai, T. Hattori, N. Higa, T. D. Matsuda, Y. Haga, R. E. Walstedt, and H. Harima, Odd-parity electronic multipolar ordering in URu_2Si_2: Conclusions from Si and Ru NMR measurements, Phys. Rev. B **97**, 235142 (2018).

[15] N. Shah, P. Chandra, P. Coleman, and J. A. Mydosh, Hidden order in URu_2Si_2, Phys. Rev. B **61**, 564 (2000).

[16] V. P. Mineev and M. E. Zhitomirsky, Interplay between spin-density wave and induced local moments in URu_2Si_2, Phys. Rev. B **72**, 014432 (2005).

[17] K. Haule and G. Kotliar, Complex Landau-Ginzburg theory of the hidden order in URu_2Si_2, Europhys. Lett. **89**, 57006 (2010).

[18] P. Chandra, P. Coleman, and R. Flint, Hastatic order in URu_2Si_2: Hybridization with a twist, Phys. Rev. B **91**, 205103 (2015).

[19] M. B. Walker, W. J. L. Buyers, Z. Tun, W. Que, A. A. Menovsky, and J. D. Garrett, Nature of the Order Parameter in the Heavy-Fermion System URu_2Si_2, Phys. Rev. Lett. **71**, 2630 (1993).

[20] S. Takagi, S. Ishihara, M. Yokoyama, and H. Amitsuka, Symmetry of the hidden order in URu_2Si_2 from nuclear magnetic resonance studies, J. Phys. Soc. Jpn. **81**, 114710 (2012).

[21] H. Ikeda, M.-T. Suzuki, R. Arita, T. Takimoto, T. Shibauchi, and Y. Matsuda, Emergent rank-5 nematic order in URu_2Si_2, Nat. Phys. **8**, 528 (2012).

[22] D. D. Khalyavin, S. W. Lovesey, A. N. Dobrynin, E. Ressouche, R. Ballou, and J. Flouquet, Symmetry-protected hidden order and magnetic neutron Bragg diffraction by URu_2Si_2, J. Phys.: Condens. Matter **26**, 046003 (2014).

[23] M.-T. Suzuki and H. Ikeda, Multipole order and global/site symmetry in the hidden-order phase of URu_2Si_2, Phys. Rev. B **90**, 184407 (2014).

[24] W. Knafo, F. Duc, F. Bourdarot, K. Kuwahara, H. Nojiri, D. Aoki, J. Billette, P. Frings, X. Tonon, E. Lelièvre-Berna, J. Flouquet, and L.-P. Regnault, Field-induced spin-density wave beyond hidden order in URu_2Si_2, Nat. Commun. **7**, 13075 (2016).

[25] Y. L. Wang, G. Fabbris, D. Meyers, N. H. Sung, R. E. Baumbach, E. D. Bauer, P. J. Ryan, J.-W. Kim, X. Liu, M. P. M. Dean, G. Kotliar, and X. Dai, On the possibility to detect multipolar order in URu_2Si_2 by the electric quadrupolar transition of resonant elastic x-ray scattering, Phys. Rev. B **96**, 085146 (2017).

[26] M.-T. Suzuki, H. Ikeda, and P. M. Oppeneer, First-principles theory of magnetic multipoles in condensed matter systems, J. Phys. Soc. Jpn. **87**, 041008 (2018).

[27] See Supplemental Material at http://link.aps.org/supplemental/10.1103/PhysRevB.98.165118 for the animated image of the $4/mmm$ configuration of 16 magnetic moments.

[28] V. M. Dubovik and V. V. Tugushev, Toroid moments in electrodynamics and solid-state physics, Phys. Rep. **187**, 145 (1990).

[29] N. Spaldin, M. Fiebig, and M. Mostovoy, The toroidal moment in condensed-matter physics and its relation to the magnetoelectric effect, J. Phys.: Condens. Matter **20**, 434203 (2008).

[30] Yu. V. Kopaev, Toroidal ordering in crystals, Phys. Usp. **52**, 1111 (2009).

[31] Yu. I. Sirotin and M. P. Shaskolskaya, *Fundamentals of Crystal Physics* (Mir, Moscow, 1982).

[32] Bilbao Crystallographic Server, http://www.cryst.ehu.es/.

[33] J. M. Perez-Mato, S. V. Gallego, E. S. Tasci, L. Elcoro, G. de la Flor, and M. I. Aroyo, Symmetry-based computational tools for magnetic crystallography, Annu. Rev. Mater. Res. **45**, 217 (2015).

[34] S. G. Porsev, Quadrupole toroidal moment of positronium, Phys. Rev. A **49**, 5105 (1994).

[35] E. Mereghetti, J. de Vries, R. G. E. Timmermans, and U. van Kolck, Toroidal quadrupole form factor of the deuteron, Phys. Rev. C **88**, 034001 (2013).

[36] C. G. Gray, G. Karl, and V. A. Novikov, Magnetic multipolar contact fields: The anapole and related moments, Am. J. Phys. **78**, 936 (2010).

[37] QUANTUM ESPRESSO, http://www.quantum-espresso.org/.

[38] P. Giannozzi, S. Baroni, N. Bonini, M. Calandra, R. Car, C. Cavazzoni, D. Ceresoli, G. L. Chiarotti, M. Cococcioni, I. Dabo, A. Dal Corso, S. de Gironcoli, S. Fabris, G. Fratesi, R. Gebauer, U. Gerstmann, C. Gougoussis, A. Kokalj, M. Lazzeri, L. Martin-Samos, N. Marzari, F. Mauri, R. Mazzarello, S. Paolini, A. Pasquarello, L. Paulatto, C. Sbraccia, S. Scandolo, G. Sclauzero, A. P. Seitsonen, A. Smogunov, P. Umari, and R. M. Wentzcovitch, QUANTUM ESPRESSO: A modular and open-source software project for quantum simulations of materials, J. Phys.: Condens. Matter **21**, 395502 (2009).

[39] J. P. Perdew and Y. Wang, Accurate and simple analytic representation of the electron-gas correlation energy, Phys. Rev. B **45**, 13244 (1992).

[40] J. P. Perdew, J. A. Chevary, S. H. Vosko, K. A. Jackson, M. R. Pederson, D. J. Singh, and C. Fiolhais, Atoms, molecules, solids, and surfaces: Applications of the generalized gradient approximation for exchange and correlation, Phys. Rev. B **46**, 6671 (1992).

[41] J. P. Perdew, K. Burke, and M. Ernzerhof, Generalized Gradient Approximation Made Simple, Phys. Rev. Lett. **77**, 3865 (1996).

[42] Z. Wu and R. E. Cohen, More accurate generalized gradient approximation for solids, Phys. Rev. B **73**, 235116 (2006).

[43] A. D. Becke, Density-functional exchange-energy approximation with correct asymptotic behavior, Phys. Rev. A **38**, 3098 (1988).

[44] J. P. Perdew, Density-functional approximation for the correlation energy of the inhomogeneous electron gas, Phys. Rev. B **33**, 8822 (1986).

[45] J. P. Perdew and A. Zunger, Self-interaction correction to density-functional approximations for many-electron systems, Phys. Rev. B **23**, 5048 (1981).

[46] H. J. Monkhorst and J. D. Pack, Special points for Brillouin-zone integrations, Phys. Rev. B **13**, 5188 (1976).

[47] N. Marzari, D. Vanderbilt, A. De Vita, and M. C. Payne, Thermal Contraction and Disordering of the Al(110) Surface, Phys. Rev. Lett. **82**, 3296 (1999).

[48] See Supplemental Material at http://link.aps.org/supplemental/10.1103/PhysRevB.98.165118 for details of the *ab initio* simulations.

[49] K. O. Kvashnina, H. C. Walker, N. Magnani, G. H. Lander, and R. Caciuffo, Resonant x-ray spectroscopy of uranium intermetallics at the $M_{4,5}$ edges of uranium, Phys. Rev. B **95**, 245103 (2017).

[50] H. Amitsuka, M. Yokoyama, S. Miyazaki, K. Tenya, T. Sakakibara, W. Higemoto, K. Nagamine, K. Matsuda, Y. Kohori, and T. Kohara, Hidden order and weak antiferromagnetism in URu_2Si_2, Physica B (Amsterdam) **312-313**, 390 (2002).

[51] See Supplemental Material at http://link.aps.org/supplemental/10.1103/PhysRevB.98.165118 for the animated images of the calculated magnetization distributions in the unit cells of the P_I4/mmm and $I4/mmm$ phases.

[52] L. Nordström and D. J. Singh, Noncollinear Intra-Atomic Magnetism, Phys. Rev. Lett. **76**, 4420 (1996).

[53] L. M. Sandratskii, Noncollinear magnetism in itinerant-electron systems: Theory and applications, Adv. Phys. **47**, 91 (1998).

[54] F. Bultmark, Distorted space and multipoles in electronic structure calculations, Doctoral thesis, Digital Comprehensive Summaries of Uppsala Dissertations from the Faculty of Science and Technology, 2009.

[55] P.-W. Ma and S. L. Dudarev, Constrained density functional for noncollinear magnetism, Phys. Rev. B **91**, 054420 (2015).

[56] A. V. Tsvyashchenko, V. A. Sidorov, A. E. Petrova, L. N. Fomicheva, I. P. Zibrov, and V. E. Dmitrienko, Superconductivity and magnetism in noncentrosymmetric RhGe, J. Alloys Compd. **686**, 431 (2016).

[57] B. Fauqué, Y. Sidis, V. Hinkov, S. Pailhès, C. T. Lin, X. Chaud, and P. Bourges, Magnetic Order in the Pseudogap Phase of High-T_C Superconductors, Phys. Rev. Lett. **96**, 197001 (2006).

[58] H. A. Mook, Y. Sidis, B. Fauqué, V. Balédent, and P. Bourges, Observation of magnetic order in a superconducting $YBa_2Cu_3O_{6.6}$ single crystal using polarized neutron scattering, Phys. Rev. B **78**, 020506 (2008).

[59] Y. Li, V. Balédent, N. Barišić, Y. Cho, B. Fauqué, Y. Sidis, G. Yu, X. Zhao, P. Bourges, and M. Greven, Unusual magnetic order in the pseudogap region of the superconductor $HgBa_2CuO_{4+\delta}$, Nature (London) **455**, 372 (2008).

[60] Y. Li, V. Balédent, N. Barišić, Y. Cho, Y. Sidis, G. Yu, X. Zhao, P. Bourges, and M. Greven, Magnetic order in the pseudogap phase of $HgBa_2CuO_{4+\delta}$ studied by spin-polarized neutron diffraction, Phys. Rev. B **84**, 224508 (2011).

[61] L. Mangin-Thro, Y. Sidis, P. Bourges, S. De Almeida-Didry, F. Giovannelli, and I. Laffez-Monot, Characterization of the intra-unit-cell magnetic order in $Bi_2Sr_2CaCu_2O_{4+\delta}$, Phys. Rev. B **89**, 094523 (2014).